scientific reports

Check for updates

OPEN

Study of autocorrelations and uncertainties applied to patients with Parkinson's disease

Florêncio Mendes Oliveira Filho[1,3]✉, Ed Frank dos Santos Silva[1,3], Sanval Ebert de Freitas Santos[1,3], Alex Álisson Bandeira Santos[1,3] & Gilney Figueira Zebende[2,3]

The control of Levodopa (L-dopa) in Parkinson's patients receiving chronic deep brain electrical stimulation (with an implant of an electrode into sub-cortical structures) will be studied here. Our main objective is to apply the Detrended Fluctuation Analysis (DFA) method and Shannon Entropy (*H*) in order to study the speed of tremor recorded in 16 patients with Parkinson's disease. These Parkinson's patients were divided into two groups (High Amplitude tremor and Low Amplitude tremor), and basically with two conditions of deep brain stimulation (on–off) and two conditions of L-dopa (on–off). These conditions (on–off) have a clear influence on the α_{DFA} exponent and the Shannon Entropy respectively. In this sense, the auto-correlation exponent gives us information whether or not there is persistence in the signal produced by the Parkinsonian rest tremor, mainly differentiating those in Low and High Amplitude, or even identifying behavior change with a typical time scale. However, the Shannon Entropy gives us information about the uncertainty in the position of Parkinsonian rest tremor. In this way, a high value of *H* informs us that we have a high uncertainty in the signal of this tremor. Therefore, by combining these two techniques we have a better view of the (signal/noise) effects of deep brain stimulation and L-dopa (medication) in all patients with Parkinson's disease, and thus helping to make a better analysis of this health problem, and with the possibility of supplementation in the Unified Parkinson's Disease Rating Scale and Tremor Rating Scale, identifying fluctuation patterns on different time scales, the nature of the tremor, and its evolution over time.

Keywords L-dopa, Detrended fluctuation analysis, Shannon entropy and uncertainty

Surgical procedures in specific regions of the brain, particularly those involving Deep Brain Stimulation (DBS), are commonly used to treat neurological disorders[1–5]. These procedures are performed to treat neurological disorders, specifically movement disorders in patients with Parkinson's disease in a progressive condition and without a definitive cure[6–9]. Each area of the brain with a specific function plays a crucial role in regulating movements, tremors, rigidity and bradykinesia (slowness of movement), exemplified by the internal Globus Pallidus area. In regions such as the ventro-intermediate nucleus of the thalamus, brain stimulation is applied to treat patients with neurological disorders that cause involuntary tremors in the hands and, in some cases, other parts of the body. Brain stimulation in the subthalamic nucleus area aims to improve the condition of patients with advanced stage Parkinson's disease[10–15]. For a Parkinson's patient to be considered a surgical candidate, some theoretical measures are regarded before implanting the sensor. Persistent motor symptoms in response to medication, with motor fluctuations or significant side effects. It is important to highlight that these measures may vary depending on the clinical case and specific medical recommendations[16,17]. Monitoring the response of patients with implanting an electrode into subcortical structures for long-term stimulation at frequencies greater than 100 Hz, located in the Ventro-intermediate nucleus of the thalamus (Vim), Globus Pallidus internus (GPi), and Subthalamic nucleus (STN) regions involves several methodologies, see Fig. 1.

This includes clinical assessment of symptoms, progression of the neurological condition over time, scales to measure specific symptoms such as tremors, rigidity and bradykinesia, symptom diaries to track their severity and impact on quality of life, imaging tests such as magnetic resonance imaging or computed tomography to

[1]Computer Engineering, SENAI CIMATEC UNIVERSITY, Salvador, Brazil. [2]State University of Feira de Santana, Bahia, Brazil. [3]Florêncio Mendes Oliveira Filho, Ed Frank dos Santos Silva, Sanval Ebert de Freitas Santos, Alex Álisson Bandeira Santos and Gilney Figueira Zebende those have contributed equally to this work. ✉email: florenciofh@yahoo.com.br

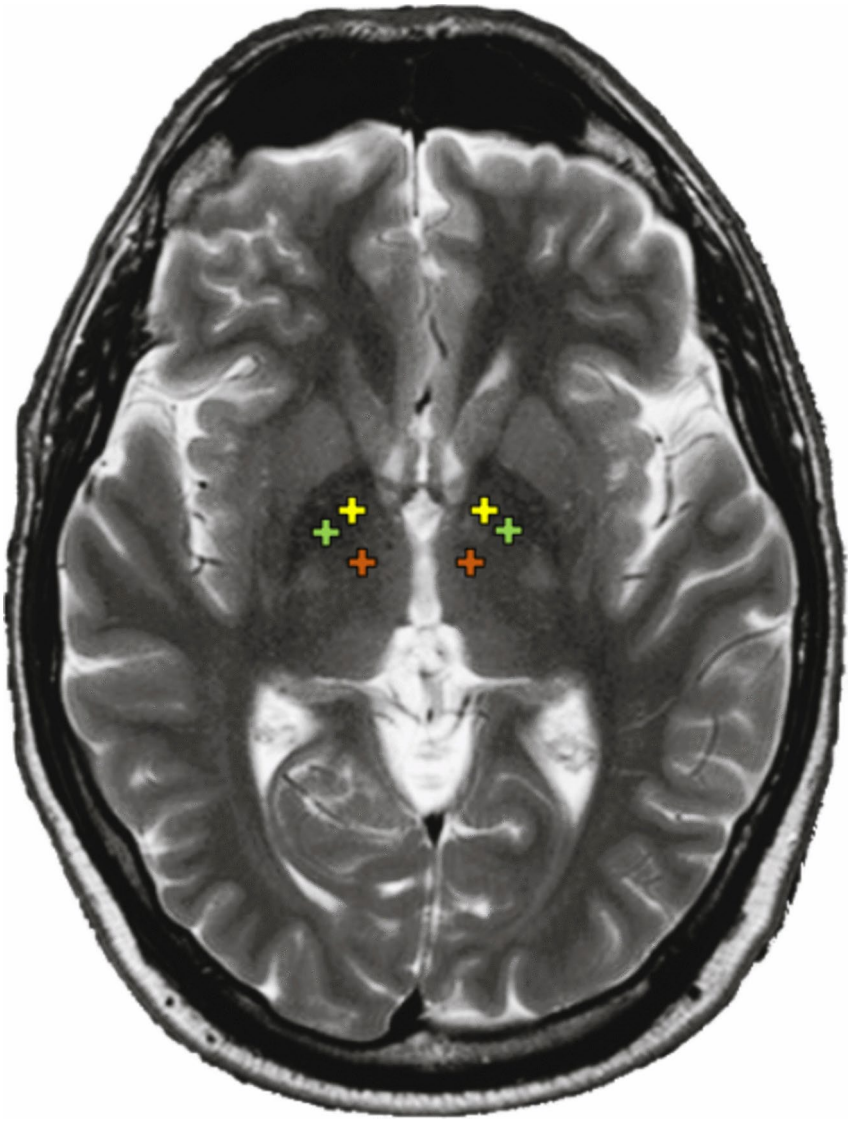

Fig. 1. Illustrative image with a plan view of the subcortical structures of the large synapses that received the implants with the: (a) Globus Pallidus interna (GPi) (green cross), Ventro-intermediate nucleus of the thalamus (Vim) (yellow cross), and the Subthalamic nucleus (STN) (orange cross).

evaluate structural changes in the brain before and after sensor implantation. Specific tests may also be conducted to assess the patient's motor, cognitive, or sensory function[18,19].

As a support tool to assess the extent of symptom severity in Parkinson's, the Unified Parkinson's Disease Rating Scale (UPDRS) and the Tremor Rating Scale (TRS) scales stand out[20]. With different purposes, UPDRS has a larger domain and covers more aspects of the disease, while TRS focuses only on assessing tremor. For the medical field, both scales contribute to the progressive monitoring of symptoms over time and, above all, can contribute to decision-making about the best treatment for each patient. It is important to highlight that both the UPDRS and the TRS need to take into account the subjectivity of reading and the technical dependence of the professional who evaluates them[21]. The UPDRS, frequently used in clinical trials and research, is divided into parts assessing mental state, behavior, mood, activity of daily living and motor examination, while the TRS is a five-point scale where 0 means absence of tremor and varying in increasing levels of severity, with level 4 being the highest[18,19].

Patients who have received brain implants in regions with a large accumulation of nerve neurons and who are being treated with L-dopa are closely monitored by a specialized medical team. Monitoring includes regular assessments of the clinical status and management of Parkinson's disease symptoms, adjustments to L-dopa as needed to optimize treatment and minimize side effects, and programming and adjustment of DBS devices to provide optimal therapy. The clinical response and DBS parameters are monitored and adapted over time to ensure the best therapeutic result[22–24].

Given this context, the conditions of the carriers, the subjectivity in the scales and the control in the adjustment of L-dopa, we propose in this research to evaluate a database available on *PhysioNet* data-bank[25],

containing recordings of resting tremor speed in 16 individuals with Parkinson's who received high-frequency DBS, unilaterally or bilaterally, in the GPi, Vim and STN regions[26,27].

In this sense, our objective here is to analyze the time-series generated from the sensor in response to the stimulus of each individual through the auto-correlation of the Detrended Fluctuation Analysis (DFA) method and the information theory proposed by Claude Shannon. Our results show that this strategy can be applied to complement the understanding of the response to L-dopa, as well as a complementary metric in the analysis of Parkinsonian tremor. To achieve this objective, we present below the development of this paper.

Data bank and methods

Data bank

The database, under Open Data Commons Attribution License (ODC-By) v1.0, was obtained from the rest tremor velocity in the index finger of 16 patients with Parkinson's disease who receive chronic high-frequency electrical DBS either uni or bi-laterally within one of three targets: Vim (**3**), GPi (**7**), or STN (**6**) (see Fig. 2). Our data were downloaded from *PhysioNet databank*[25]. In this test, DBS was implanted through a surgical procedure in three subcortical structures of large synapses in the brain for long-term stimulation at frequencies greater than 100Hz[6].

Among the 16 patients with Parkinson's disease, eleven men and five women were tested, subdivided into two groups:

- **group 1**: Subjects 1-8 with High Amplitude tremor who are receiving DBS to relieve tremor (average age 58.5 years) with: Vim (**3**), GPi (**2**), and STN (**3**);
- **group 2**: Subjects 9-16 with Low Amplitude tremor who are receiving DBS to relieve other symptoms such as rigidity or dyskinesias (average age 52.8 years) with: GPi (**5**), and STN (**3**).

All patients were in stable clinical condition at the moment of the tests. For example, minimal dopaminergic therapy ranging from 300 to 1200 mg per day of L-dopa without the use of any other medication related to parkinsonian pathology at least 12 hours before the start of the tests and were not allowed to have more than one morning coffee on the two test days. Finally, the the tremor was recorded for approximately 60s under various conditions (see Fig. 3 as an example), i.e.:

- Two conditions of DBS (**on–off**) and two conditions of L-dopa (**on–off**), with 55 recordings of approx 60s each;
- Every 15min when DBS was stopped for 60min (L-dopa **off**), with 46 recordings of approx 60s each.

At the end of test, we have the following structure for file naming:

- 2 character patient identification: stimulation target, v (Vim), s (STN), g (GPi) and patient number (1-16);
- 1 character tremor type: r (resting tremor);

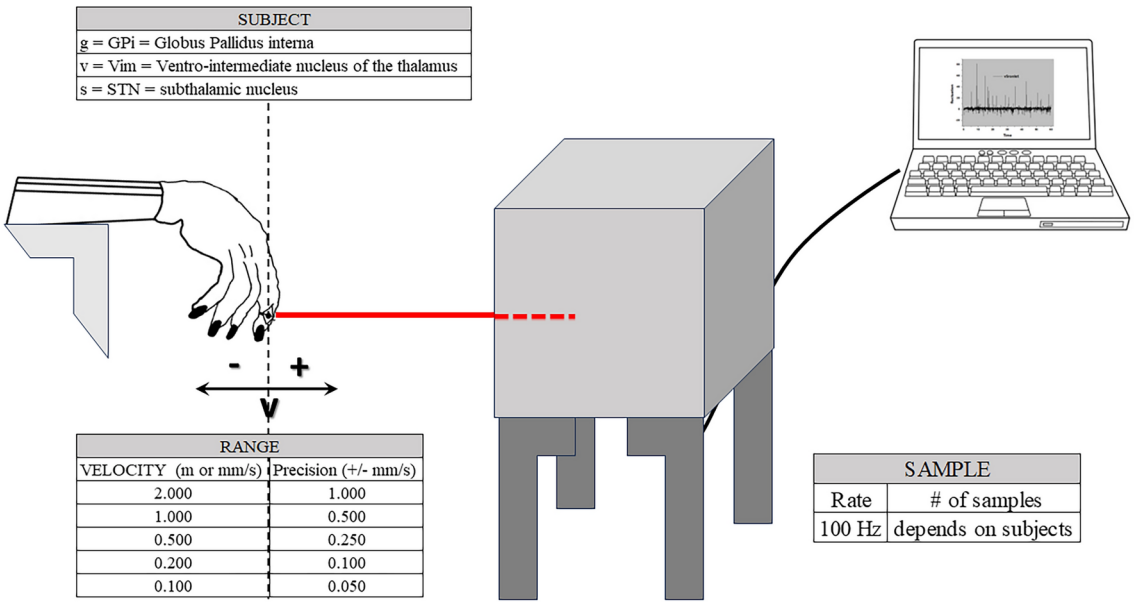

Fig. 2. Illustrative diagram for the Parkinsonian rest tremor velocity. The raw data is stored on a computer, obtained using a low intensity velocity-transducing laser that was directed at a piece of reflective paper on the patients index finger tip, with the output voltage (in the personal computer) proportional to the velocity of the finger.

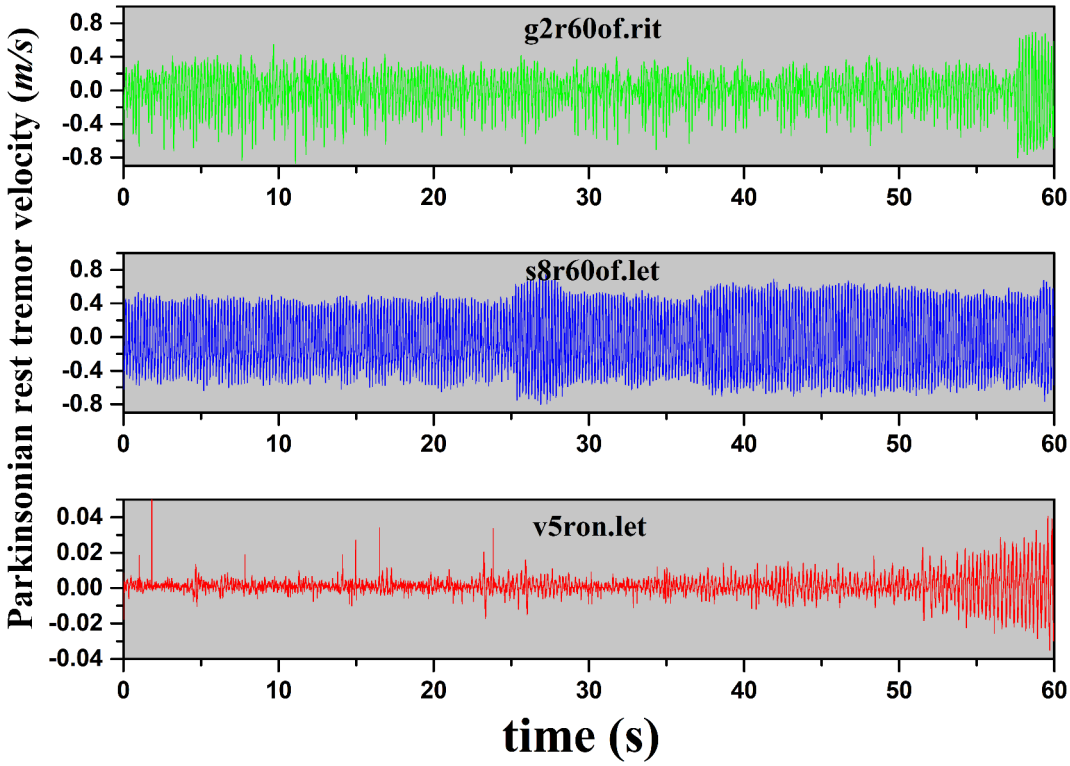

Fig. 3. Parkinsonian rest tremor velocity applied in three different situations. Following the filename structure in[25] we have: **g2r60of.rit**: stimulation target GPi, patient 2, resting tremor, 60min since the stimulation was stopped, L-dopa condition **off**, and right index finger tremor. **s8r60of.let**: stimulation target STN, patient 8, resting tremor, 60m since the stimulation was stopped, L-dopa condition **off**, and left index finger tremor. **v5ron.let**: stimulation target Vim, patient 5, resting tremor, L-dopa condition **on**, and left index finger tremor.

- 1 character DBS condition: e (effective) ($>$ 100Hz), o (no stimulation) (optional). 2 character time since stimulator arrest: if a 2 digit number follows the DBS condition, it indicates the number of minutes since the stimulation was stopped;
- 1 character medication condition: n (L-dopa **on**), f (L-dopa **off**);
- 3 character extension indicates the side tested: let (left index finger tremor), rit (right index finger tremor).

Information about the 16 patients who received DBS by: the description by groups, the identification of the patient, the target region (Vim, GPi, STN), age at the time of the test and gender, condition (universely or bilaterally), specific frequencies and year of diagnosis. All results steps take into account DBS (**on–off**) and Medication (L-dopa **on–off**), also taking into account the time of 15min when DBS was interrupted for 60min (L-dopa **off**). For the "no medication" condition, the patient had not taken any L-dopa for at least 12 hours. For the "medication **on**" condition, the patient took 150% of a daily dose of Modopar and began after the neurophysiologist identified the effect of the L-dopa ($\sim$ 40min).

More details about the patient description with Parkinson's disease can be see on the web page: https://physionet.org/content/tremordb/1.0.0/

Now, we briefly present the methods for analyzing the signals captured from tremors in these 16 patients, immediately below.

Methods

Detrended fluctuation analysis

In short, we describe the DFA method, proposed by Peng et al.[28], as a statistical method applied in auto-correlation analysis. In this sense, consider a time-series $\{u_i\}$ (eletrical potencial), with $i = 1, \cdots, N_{max}$ (time-series N_{max} length). The next step to understanding the *DFA* method, consists of determining the deviations in relation to the mean value $\langle u \rangle$, and thus obtaining the new integrated time-series, by:

$$y(k) = \sum_{i=1}^{k} [u_i - \langle u \rangle] \tag{1}$$

with $k = 1, \ldots, N_{max}$. The integrated time-series, $y(k)$, is divided in equal-sized boxes n. For each box of size n, a polynomial of degree 1 is obtained by the least squares method. This fit provides the local trend, $y_n k$, in each

box. Now, the integrated time-series, $y(k)$, is subtracted by $y_n k$ in each box of size n (time scale). Afterwards, the mean square root fluctuation function, $F_{DFA}(n)$, is calculated by:

$$F_{DFA}(n) = \sqrt{\frac{1}{N_{max}} \sum_{k=1}^{N_{max}} [y(k) - y_n(k)]^2} \tag{2}$$

The above calculation is repeated for a wide of time scales, that is, $4 \leq n \leq \frac{N_{max}}{4}$. If, F_{DFA}, follow a power-law as a function of the time scale n, thus:

$$F_{DFA}(n) \sim n^{\alpha_{DFA}} \tag{3}$$

with α_{DFA} defined as the auto-correlation exponent, or the long-range correlation indicator, see Table 1 and[29,30] for more details.

We can mention some more articles that applied the DFA method to analyze EEG signals, including[31–37].

Shannon entropy and uncertainty

In the information theory, the Shannon Entropy is a fundamental concept based on the basic notions of probability in a finite sample space. It is a measure of uncertainty in a system. The measurement takes into account that the greater the entropy of the system, the greater its uncertainty[38–40]. The concept of Shannon Entropy was applied in the most diverse areas of knowledge (interdisciplinary method), such as: information science[41,42], biology[43,44], medicine[45–48], ecology[49], economics[50], linguistics[51], among many other papers.

Specifically, based on the classical information theory, given a discrete random variable X, we can define the Shannon Entropy as:

$$H(X) = -\sum_{x \in X} p_x log_b\, p_x \tag{4}$$

where $\sum$ denotes the sum over the possible values of x, and b is the base of the logarithm applied, with common values, which are: $b = 2$ (bits), $b = \exp$ (nats), and $b = 10$ (bans)[52]. The Shannon Entropy depends only on the distribution of X, and has the following characteristics:

- The maximum value is attained by a uniformly distributed random variable;
- When the occurrence of a given information becomes more likely than others, in the repertoire, the entropy decreases;
- When there is certainty about the information, the entropy is zero.

The Shannon Entropy, H, is normalized here and range between 0 and 1. A high Shannon Entropy means a high degree of uncertainty (less information) in this time-series, while low entropy means a lower uncertainty (more information). To study the values of the signals obtained by tremors recording, in this paper we converted each index finger resting tremor speed time-series into an adaptive series for transformation, ou seja, we replace the "negative" and "dot" signs with a representative number (minus sign (–) for 45 and the dot poit (.) for 46. With these substitutions in hand, we convert the series to a new binary sequence (0 and 1), generating a new time-series. After, we applied the model described by Eq. (4).

After this theoretical explanation we introduce the results about DFA method and Shannon Entropy (uncertainty of information) immediately below.

Results

With the aim of analyzing the effects of DBS and L-dopa (medication) on 16 patients with Parkinson's disease through recordings of the speed of resting tremor of the finger indicator (left/right) (see Fig. 2) on three brain regions (see Fig. 1), here we applied the DFA method and the Shannon Entropy (information uncertainty). Therefore, each time-series with $\approx$ 60s was separated into two groups: patients classified as a Low Amplitude and patients with High Amplitude tremor, as seen below (Figs. 4 and 5 and Tables).

We start the DFA results for that case in which the patients were tested with L-dopa **off** and DBS **off** for 15min (Fig. 4a), with 8 (eight) curves for Low Amplitude and 3 (three) curves for High Amplitude tremor. We can see

DFA exponent	Type of signal
$\alpha_{DFA} < 0.5$	Long-range anti-persistent
$\alpha_{DFA} \simeq 0.5$	Uncorrelated (white noise)
$\alpha_{DFA} > 0.5$	Long-range persistent
$\alpha_{DFA} \simeq 1$	$1/f$ noise
$\alpha_{DFA} > 1$	Non-stationary
$\alpha_{DFA} \simeq 3/2$	Brownian noise

Table 1. DFA exponent and its type of signal.

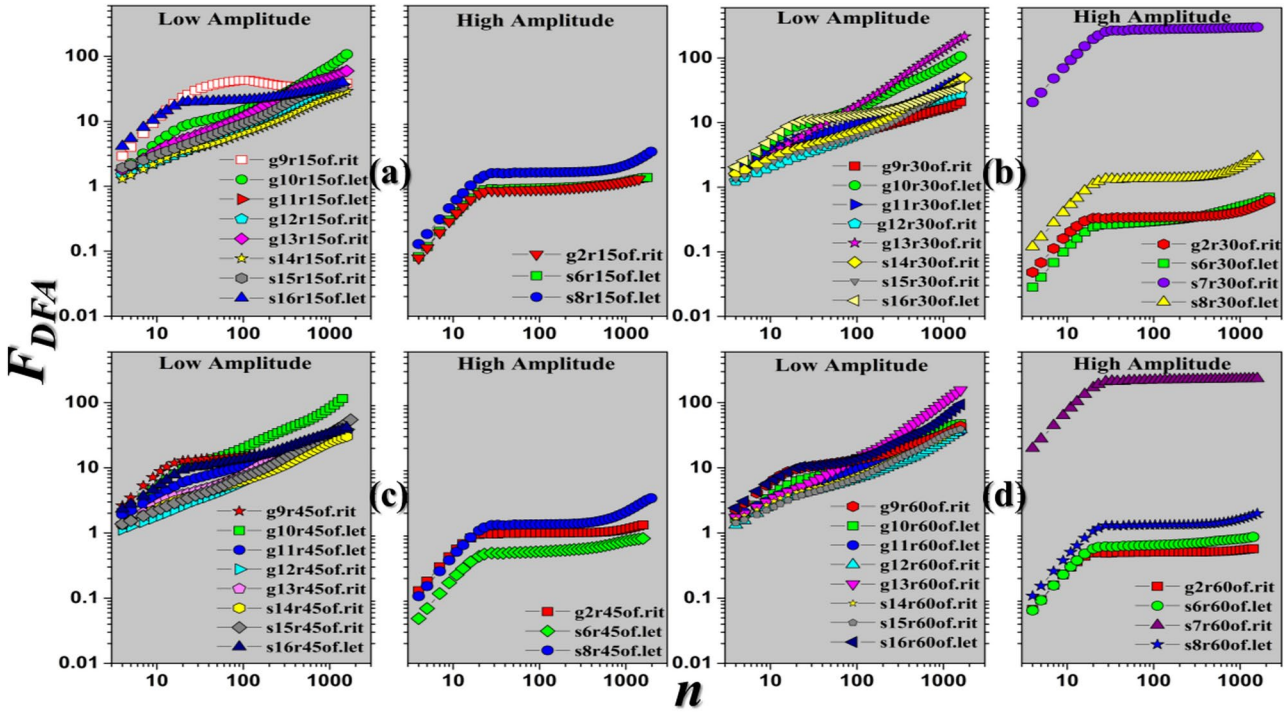

Fig. 4. F_{DFA} as a funtion of the time scale n for L-dopa **off** and DBS **off** for: (**a**) 15min, (**b**) 30min, (**c**) 45min, and (**d**) 60min. On the left, we have the results for patients with Low Amplitude, while on the right is shown the results for patients with High Amplitude tremor.

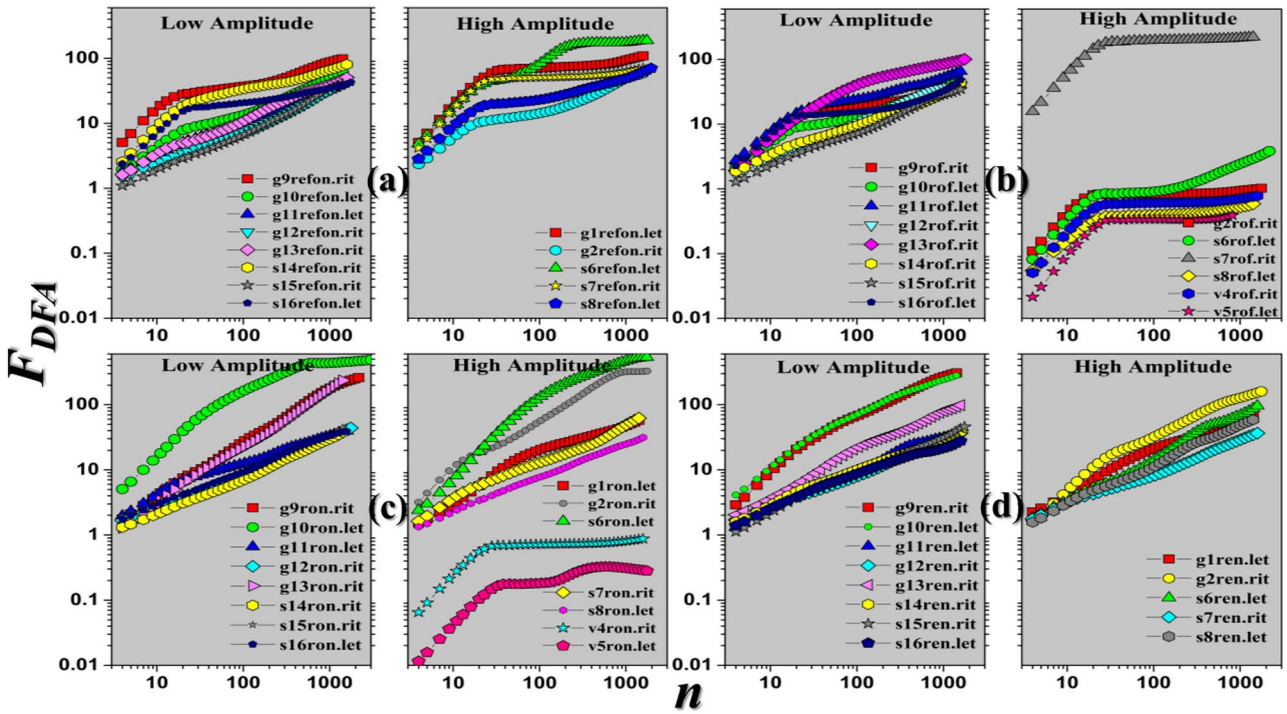

Fig. 5. F_{DFA} as a funtion of the time scale n for: (**a**) DBS **off** and L-dopa **off**, (**b**) DBS **on** and L-dopa **off**, (**c**) DBS **off** and L-dopa **on**, and (**d**) DBS **on** and L-dopa **on**. On the left, we have the results for patients with Low Amplitude, while on the right, is shown the results for patients with High Amplitude tremor.

that the fluctuation function, F_{DFA}, for Low Amplitude had a higher value if compared to those classified in High Amplitudes. The reason for this fact comes from the difference between the intensities and amplitudes, that is, the greater the oscillation amplitude, the smaller is the root mean square fluctuation. Furthermore, except for g9r15of.rit and s16r15of.let patients there is a power-law governing the test for Low Amplitude group, which is not seen for the case of High Amplitude, where there is a clear behavior transition in the F_{DFA} function around $n \approx 20$.

How there is a behavior transition in $F_{DFA}(n)$ function, and based on[30], we calculate α_{DFA} between these time scales: $4 \leq n < 20$ (small time scales), $20 < n < 800$ (medium time scales), and $n > 800$ (large time scales). The values found for the α_{DFA} exponent, as well as, the Shannon Entropy H are presented below in all Tables.

Specifically, the results for α_{DFA} and H for DBS **off** for 15min and L-dopa **off**, are presented in the Table 2.

In the Table 2, group 1 (High Amplitude) we can see that for:

- Small time scales, $4 \leq n < 20$, $\alpha_{DFA} > 1.4$;
- Medium time scales, $20 < n < 800$, $\alpha_{DFA} \approx 0$ (anti-persistence);
- Large time scales, $n > 800$, α_{DFA} varies from anti to persistent case, depending on the patient;

For the group 2 (Low Amplitude), in general there is a power-law with $\alpha_{DFA} \approx 0.5$, except for the patients g9r15of.rit, g10r15of.let, and s16r15of.let, who present $\alpha_{DFA} \approx 1.00$ for small time scales. Also, we identified that there is a maximum uncertainty for all patients in the group 1 (High Amplitude), regarding the value of $H = 1.00$ (last column in the table). The same thing cannot be said about the group 2 (Low Amplitude), because $0.46 \leq H \leq 0.75$ (medium to high uncertainty).

The next step was to analysis the patients tested with DBS **off** for 30min and L-dopa **off** (Fig. 4b), with eight (8) curves for Low Amplitude and four (4) curves for High Amplitude tremor. We identify the same pattern as the case seen previously for DBS **off** for 15min, except for s7r30of.rit which, although there is a transition in $n \approx 20$, display F_{DFA} of the order of those found in Low Amplitudes, see Table 3 for more details.

Continuing our analysis, for the case where DBS was **off** for 45min (Fig. 4c), as well as, for DBS **off** for 60min (Fig. 4d)with L-dopa **off**, the results found for the α_{DFA} exponent and H are equivalent to those found previously, see Tables 4 and 5.

Again, as in the case with L-dopa **off** and DBS **off** for 30min, the patient 7 group 1 (High Amplitude) identified here by s7r60of.rit has values of F_{DFA} comparable to those of group 2 (Low Amplitudes), also with a clear transition of behavior at $n \simeq 20$.

For that cases where there is no characteristic time for DBS (**on–off**), i.e., a time since stimulator arrest was stopped, the results for $F_{DFA} \times n$ can be found in the Fig. 5 with α_{DFA} exponent and H values presented in the Tables 7, 6, 8, and 9 respectively.

In this case we have four possibilities, in other words: DBS **off** and L-dopa **off**, DBS **on** and L-dopa **off**, DBS **off** and L-dopa **on**, and DBS **on** and L-dopa **on**. For the this case, DBS **off** and L-dopa **off**, Fig. 5a, we have eight (8) Low Amplitude and six (6) High Amplitude tremor curves, the results can be found in Table 6 for both α_{DFA} and H.

This results show that this situation is closer to the one where DBS was turned off for a period of 60min, see Fig. 4d. Now for DBS **on** with L-dopa **off**, Fig. 5b, there are five (5) patients with High Amplitude and eight (8) patients with Low Amplitude tremor curves. In this case, no major differences in results between Low and High Amplitudes are identified, however we can intensify a behavior transition in $n \approx 20$ in some cases. The values for, α_{DFA} and H, with DBS **on** and L-dopa **off** can be found in the Table 7.

In this table it can be seen that the mean value of auto-correlation exponent on small time scales, $n < 20$, is $\langle \alpha_{DFA} \rangle \simeq 1.20$, that is, it is slightly smaller than those obtained previously (DBS **on** for 15, 30, 45, and 60min),

	Subjects		DFA exponent		H
		$4 \leq n < 20$	$20 < n < 800$	$n > 800$	
High Amp.	g2r15of.rit	1.44 ± 0.04	0.09 ± 0.01	0.26 ± 0.02	**1.00**
	s6r15of.lef	1.44 ± 0.04	0.09 ± 0.01	0.26 ± 0.01	**1.00**
	s8r15of.lef	1.46 ± 0.03	0.05 ± 0.01	0.67 ± 0.01	**1.00**
Low Amp.	g9r15of.rit	1.15 ± 0.05	0.18 ± 0.02	0.01 ± 0.01	**0.65**
	g10r15of.lef	0.97 ± 0.02	0.35 ± 0.01	0.79 ± 0.01	**0.59**
	g11r15of.lef	0.52 ± 0.01	✓	✓	**0.75**
	g12r15of.rit	0.53 ± 0.01	✓		**0.59**
	g13r15of.rit	0.58 ± 0.01	✓	✓	**0.65**
	s14r15of.rit	0.50 ± 0.01	✓	✓	**0.46**
	s15r15of.rit	0.52 ± 0.01	✓	✓	**0.49**
	s16r15of.lef	0.97 ± 0.04	0.16 ± 0.01	✓	**0.71**

Table 2. DFA auto-correlation exponents calculated for DBS **off** for 15min and L-dopa **off**, as reported here in the Fig. 4a. The last column show the value of the Shannon Entropy, that shows the values between 0 and 1, where 0 means absence and 1 maximum uncertainty. The checkmark (✓) means that the value of α_{DFA} is the same as the previous time scale.

	Subjects		DFA exponent		H
		$4 \leq n < 20$	$20 < n < 800$	$n > 800$	
High Amp.	g2r30of.rit	1.24 ± 0.01	0.02 ± 0.01	0.37 ± 0.01	**0.89**
	s6r30of.lef	1.22 ± 0.07	0.12 ± 0.01	0.36 ± 0.01	**0.95**
	s7r30of.rit	1.37 ± 0.03	0.02 ± 0.01	✓	**0.99**
	s8r30of.lef	1.35 ± 0.03	0.04 ± 0.04	0.74 ± 0.01	**1.00**
Low Amp.	g9r30of.rit	0.35 ± 0.01	✓	✓	**0.53**
	g10r30of.lef	0.95 ± 0.01	0.56 ± 0.01	0.75 ± 0.01	**0.58**
	g11r30of.lef	0.49 ± 0.09	✓	✓	**0.77**
	g12r30of.rit	0.49 ± 0.01	✓	✓	**0.57**
	g13r30of.rit	0.81 ± 0.01	✓	✓	**0.66**
	s14r30of.rit	0.52 ± 0.01	✓	✓	**0.47**
	s15r30of.rit	0.53 ± 0.01	✓	✓	**0.46**
	s16r30of.lef	1.00 ± 0.02	0.24 ± 0.01	0.35 ± 0.01	**0.60**

Table 3. DFA auto-correlation exponents calculated for DBS **off** for 30min and L-dopa **off**, as reported here in the Fig. 4b. The last column show the value of the Shannon Entropy. The checkmark (✓) means that the value of α_{DFA} is the same as the previous time scale.

	Subjects		DFA exponent		H
		$4 \leq n < 20$	$20 < n < 800$	$n > 800$	
High Amp.	g2r45of.rit	1.27 ± 0.06	0.02 ± 0.01	0.28 ± 0.01	**1.00**
	s6r45of.let	1.39 ± 0.04	0.09 ± 0.01	0.24 ± 0.01	**0.98**
	s8r45of.let	1.46 ± 0.03	0.06 ± 0.01	0.69 ± 0.01	**1.00**
Low Amp.	g9r45of.rit	1.00 ± 0.04	0.15 ± 0.01	0.40 ± 0.01	**0.64**
	g10r45of.let	0.99 ± 0.01	0.53 ± 0.01	0.93 ± 0.01	**0.60**
	g11r45of.let	0.73 ± 0.01	0.44 ± 0.01	0.26 ± 0.03	**0.77**
	g12r45of.rit	0.59 ± 0.01	✓	✓	**0.56**
	g13r45of.rit	0.55 ± 0.01	✓	✓	**0.63**
	s14r45of.rit	0.50 ± 0.01	✓	✓	**0.46**
	s15r45of.rit	0.59 ± 0.01	✓	✓	**0.45**
	s16r45of.let	0.88 ± 0.01	0.32 ± 0.01	0.45 ± 0.01	**0.59**

Table 4. DFA auto-correlation exponents calculated for DBS **off** for 45min and L-dopa **off**, as reported here in the Fig. 4c. The last column show the value of the Shannon Entropy. The checkmark (✓) means that the value of α_{DFA} is the same as the previous time scale.

showing a similar behavior from its auto-correlation with these previously mentioned. However, the value of H tends to be lower than 1.00 (lower position uncertainty), even for High Amplitudes cases, with $\langle H \rangle \simeq 0.71$.

Following our findings, in the Fig. 5c with DBS **off** and L-dopa **on**, we have the results for $F_{DFA} \times n$, totalizing eight (8) patients with Low Amplitude and seven (7) patients with High Amplitude tremor curves. Here, the results can be found in Table 8 for α_{DFA} and H.

It is observed that, with DBS **off** and the L-dopa **on**, this situation tends to lead the F_{DFA} function to appear similar values for that with Low Amplitude tremor. But, for some patients this is not true, that is, mainly in those where the sensor is located in the Ventro-intermediate nucleus of the thalamus, patients v4ron.rit and v5ron.let. From the point of view of Shannon Entropy, it is observed that the average value of H for High Amplitude is 0.65, while for Low Amplitudes 0.60 (less uncertainty in the position).

Closing all possibilities, we can see the results for DBS **on** and L-dopa **on**, Fig. 5d, with eight (8) patients in Low Amplitude and five (5) patients in High Amplitude tremor (the most complete Parkinson's treatment), with α_{DFA} and H values showing in the Table 9.

Something interesting happens and is quite visible for the case with DBS **on** and L-dopa **on**. In general, we can not see the behavior transition to F_{DFA} in time scale $n \simeq 20$, and the single power-law becomes more evident (see the values of α_{DFA} in the Table 9), with prevalence of persistence in most cases. Therefore, for the Shannon Entropy we observe that, in this most complete Parkinson's treatment, the mean value for H in High and Low Amplitude are closer (or equal), around a value of 0.61.

Discussion

In this paper we applied the DFA method and Shannon Entropy in order to study the speed of tremor recorded in patients with Parkinson's disease. These patients were divided into two groups: group 1 (with patients

	Subjects		DFA exponent		*H*
		$4 \leq n < 20$	$20 < n < 800$	$n > 800$	
High Amp.	g2r60of.rit	1.28 ± 0.06	0.02 ± 0.01	✓	**0.93**
	s6r60of.let	1.38 ± 0.05	0.08 ± 0.01	✓	**1.00**
	s7r60of.rit	1.34 ± 0.02	0.02 ± 0.01	✓	**0.94**
	s8r60of.let	1.48 ± 0.02	0.03 ± 0.01	0.41 ± 0.01	**1.00**
Low Amp.	g9r60of.rit	0.92 ± 0.04	0.29 ± 0.01	0.60 ± 0.01	**0.59**
	g10r60of.let	0.85 ± 0.01	0.45 ± 0.01	0.57 ± 0.03	**0.55**
	g11r60of.let	0.50 ± 0.01	✓	✓	**0.74**
	g12r60of.rit	0.50 ± 0.01	✓	✓	**0.62**
	g13r60of.rit	0.74 ± 0.01	✓	✓	**0.65**
	s14r60of.rit	0.50 ± 0.01	✓	✓	**0.49**
	s15r60of.rit	0.55 ± 0.01	✓	✓	**0.45**
	s16r60of.let	0.92 ± 0.04	0.44 ± 0.02	0.99 ± 0.01	**0.61**

Table 5. DFA auto-correlation exponents calculated for DBS **off** for 60min and L-dopa **off**, as reported here in the Fig. 4d. The last column show the value of the Shannon Entropy. The checkmark (✓) means that the value of α_{DFA} is the same as the previous time scale.

	Subjects		DFA exponent		*H*
		$4 \leq n < 20$	$20 < n < 800$	$n > 800$	
High Amp.	g2rof.rit	1.09 ± 0.09	0.04 ± 0.01	✓	**0.99**
	s6rof.let	1.35 ± 0.05	0.25 ± 0.02	0.56 ± 0.01	**1.00**
	s7rof.rit	1.30 ± 0.04	0.03 ± 0.01	✓	**0.94**
	s8rof.let	1.02 ± 0.03	0.10 ± 0.01	✓	**0.89**
	v4rof.rit	1.30 ± 0.06	0.05 ± 0.01	✓	**0.93**
	v5rof.lef	1.44 ± 0.04	0.02 ± 0.01	✓	**0.83**
Low Amp.	g9rof.rit	1.03 ± 0.04	0.18 ± 0.01	0.20 ± 0.01	**0.60**
	g10rof.let	0.86 ± 0.03	0.37 ± 0.01	0.58 ± 0.01	**0.59**
	g11rof.let	0.98 ± 0.03	0.31 ± 0.01	✓	**0.88**
	g12rof.rit	0.48 ± 0.01	✓	✓	**0.60**
	g13rof.rit	1.16 ± 0.02	0.47 ± 0.01	0.29 ± 0.01	**0.61**
	s14rof.rit	0.54 ± 0.01	✓	✓	**0.51**
	s15rof.rit	0.55 ± 0.01	✓	✓	**0.45**
	s16rof.let	0.99 ± 0.05	0.18 ± 0.01	0.74 ± 0.03	**0.64**

Table 6. DFA auto-correlation exponents calculated for DBS **off** and L-dopa **off**, as reported here in the Fig. 5 (b). The last column show the value of the Shannon Entropy. The checkmark (✓) means that the value of α_{DFA} is the same as the previous time scale.

enumerated from 1 to 8) with High Amplitude tremor who are receiving DBS to alleviate tremor and group 2 (with patients enumerated from 9 to 16) with Low Amplitude tremor who are receiving DBS to alleviate other symptoms such as rigidity or dyskinesias. Basically, there are two conditions of DBS (**on–off**) and two conditions of medication (L-dopa **on–off**), totaling four distinct cases (see description):

- **Case 1**: DBS **off** and L-dopa **off**: That there is a clear behavior transition at $n \simeq 20$ (small time scale), observed by α_{DFA} exponent, mainly for the group 1 (High Amplitude tremor). Also, in this case, in general $F_{DFA}(\text{Hight Amplitude}) < F_{DFA}(\text{Low Amplitude})$. The mean value for the Shannon Entropy (*H*) for High Amplitude is approximately 0.93, while for Low Amplitudes is 0.61 (less uncertainty in the laser position).
- **Case 2**: DBS **on** and L-dopa **off**: In this case, $F_{DFA}(\text{Hight Amplitude}) \approx F_{DFA}(\text{Low Amplitude})$, but, it is still possible to verify the transition of behavior around $n \simeq 20$ for the group 1 (High Amplitude tremor). The mean value for the Shannon Entropy (*H*) for High Amplitude is approximately 0.71, while for Low Amplitudes is 0.65.
- **Case 3**: DBS **off** and L-dopa **on**: Is still possible to verify the transition around $n \simeq 20$), $F_{DFA}(\text{Hight Amplitude}) \approx F_{DFA}(\text{Low Amplitude})$ (except for v4ron.rit and v5r.let patients). The mean value for the Shannon Entropy (*H*) for High Amplitude is approximately 0.65, while for Low Amplitudes is 0.60.

	Subjects		DFA exponent		*H*
		$4 \leq n < 20$	$20 < n < 800$	$n > 800$	
High Amp.	g1refon.let	1.29 ± 0.03	0.06 ± 0.01	✓	**0.76**
	g2refon.rit	0.95 ± 0.03	0.36 ± 0.01	0.45 ± 0.02	**0.69**
	s6refon.let	1.35 ± 0.01	0.51 ± 0.02	0.12 ± 0.01	**0.89**
	s7refon.rit	1.30 ± 0.05	0.07 ± 0.01	✓	**0.49**
	s8refon.let	1.04 ± 0.05	0.07 ± 0.01	✓	**0.70**
Low Amp.	g9refon.rit	1.19 ± 0.04	0.25 ± 0.01	0.35 ± 0.01	**0.75**
	g10refon.let	0.88 ± 0.01	0.46 ± 0.01	0.64 ± 0.01	**0.57**
	g11refon.let	0.50 ± 0.01	✓	✓	**0.74**
	g12refon.rit	0.56 ± 0.01	✓	✓	**0.60**
	g13refon.rit	0.56 ± 0.01	✓	✓	**0.66**
	s14refon.rit	1.31 ± 0.02	0.28 ± 0.01	✓	**0.64**
	s15refon.rit	0.61 ± 0.01	✓	✓	**0.45**
	s16refon.let	1.21 ± 0.01	0.21 ± 0.01	✓	**0.77**

Table 7. DFA auto-correlation exponents calculated for DBS **on** and L-dopa **off**, as reported here in the Fig. 5 (a). The last column show the value of the Shannon Entropy. The checkmark (✓) means that the value of α_{DFA} is the same as the previous time scale.

	Subjects		DFA exponent		*H*
		$4 \leq n < 20$	$20 < n < 800$	$n > 800$	
High Amp.	g1ron.let	0.79 ± 0.01	0.45 ± 0.01	✓	**0.49**
	g2ron.rit	1.20 ± 0.05	0.82 ± 0.01	0.08 ± 0.01	**0.71**
	s6ron.let	1.27 ± 0.01	0.79 ± 0.03	0.31 ± 0.02	**0.71**
	s7ron.rit	0.59 ± 0.02	✓	✓	**0.53**
	s8ron.let	0.52 ± 0.02	✓	✓	**0.59**
	v4ron.rit	1.23 ± 0.05	0.04 ± 0.01	✓	**0.95**
	v5ron.let	1.39 ± 0.01	0.26 ± 0.01	0.15 ± 0.02	**0.58**
Low Amp.	g9ron.rit	0.80 ± 0.01	✓	✓	**0.55**
	g10ron.let	1.27 ± 0.01	0.62 ± 0.01	0.09 ± 0.01	**0.62**
	g11ron.let	0.89 ± 0.01	0.41 ± 0.01	✓	**0.79**
	g12ron.rit	0.53 ± 0.01	✓	✓	**0.59**
	g13ron.rit	0.86 ± 0.01	✓	✓	**0.66**
	s14ron.rit	0.57 ± 0.01	✓	✓	**0.45**
	s15ron.rit	0.52 ± 0.01	✓	✓	**0.49**
	s16ron.let	0.53 ± 0.01	✓	✓	**0.62**

Table 8. DFA auto-correlation exponents calculated for DBS **off** and L-dopa **on**, as reported here in the Fig. 5 (c). The last column show the value of the Shannon Entropy. The checkmark (✓) means that the value of α_{DFA} is the same as the previous time scale.

- **Case 4**: DBS **on** and L-dopa **on**: This is the case of the most complete Parkinson's treatment. From the point of view of auto-correlation, both Low and Hight Amplitudes cases had a single power-law, $F_{DFA} \propto n^{\alpha_{DFA}}$, with $< \alpha_{DFA} >= 0.61$ (Hight Amplitude) and $< \alpha_{DFA} >= 0.59$ (Low Amplitude). Here, the mean value of *H* in High and Low Amplitude is close to 0.61.

For a better exemplification of the results and to summarize this analysis, in Fig. 6 is showing one diagram for *H* and α_{DFA} with six patients who performed these four distinct cases: (g2, s6, s8) (High Amplitude) and (g10, g13, s16) (Low Amplitude).

It is clear that for **Case 1**, DBS **off** and L-dopa **off**, $F_{DFA}(\text{Hight Amplitude}) < F_{DFA}(\text{Low Amplitude})$, that is, the greater is the amplitude of oscillation, the smaller is thee root mean square fluctuation. This effect is also reflected in the value of Shannon Entropy, the mean value of *H* for High Amplitude tends to $H = 1.0$ (maximum uncertainty), while for Low Amplitudes *H* tends to values much smaller than 1.0 (less uncertainty in the position). However, if DBS or L-dopa is **on**, there is a clear influence on the results. For example, for the **Case 2** and the **Case 3**, the value of the fluctuation function has the same order of magnitude for both cases, in Hight and Low Amplitude, and the mean value of *H* for High Amplitude tends to *H* for Low Amplitude, in other words:

- $F_{DFA}(\text{Hight Amplitude}) \approx F_{DFA}(\text{Low Amplitude})$;

	Subjects	DFA exponent	H
High Amp.	g1ren.let	0.57 ± 0.01	**0.54**
	g2ren.rit	0.70 ± 0.01	**0.69**
	s6ren.let	0.67 ± 0.01	**0.66**
	s7ren.rit	0.49 ± 0.01	**0.50**
	s8ren.let	0.61 ± 0.01	**0.64**
Low Amp.	g9ren.rit	0.74 ± 0.02	**0.62**
	g10ren.let	0.70 ± 0.02	**0.67**
	g11ren.let	0.58 ± 0.01	**0.72**
	g12ren.rit	0.49 ± 0.01	**0.63**
	g13ren.rit	0.65 ± 0.01	**0.76**
	s14ren.rit	0.49 ± 0.01	**0.44**
	s15ren.rit	0.58 ± 0.01	**0.46**
	s16ren.let	0.47 ± 0.01	**0.62**

Table 9. DFA exponent calculated for DBS **on** and L-dopa **on**, as reported here in the Fig. 5d. In this case α_{DFA} exponent is valid for all time scale. The last column show the value of the Shannon Entropy.

		case 1			case 2			case 3			case 4		
		DBS off	L-dopa off		DBS on	L-dopa off		DBS off	L-dopa on		DBS on	L-dopa on	
		H	α_{DFA1}	α_{DFA2}	H	α_{DFA1}	α_{DFA2}	H	α_{DFA1}	α_{DFA2}	H	α_{DFA1}	α_{DFA2}
group 1 Hight	g2	0.99	1.09	0.04	0.69	0.95	0.36	0.71	1.20	0.82	0.69	0.70	0.70
	s6	1.00	1.35	0.25	0.89	1.35	0.51	0.71	1.27	0.79	0.66	0.67	0.67
	s8	0.89	1.02	0.10	0.70	1.04	0.07	0.59	0.52	0.52	0.64	0.61	0.61
		$F_{DFA\_H} < F_{DFA\_L}$			$F_{DFA\_H} \approx F_{DFA\_L}$			$F_{DFA\_H} \approx F_{DFA\_L}$			$F_{DFA\_H} \approx F_{DFA\_L}$		
group 2 Low	g10	0.59	0.86	0.37	0.57	0.88	0.46	0.62	1.27	0.62	0.67	0.70	0.70
	g13	0.61	1.16	0.47	0.66	0.56	0.56	0.66	0.86	0.86	0.76	0.65	0.65
	s16	0.64	0.99	0.18	0.77	1.21	0.21	0.62	0.53	0.53	0.62	0.47	0.47

Fig. 6. Diagram of case with: DBS (**on–off**) and L-dopa (**on–off**). Six patients, three in High Amplitude (group 1) and three in Low Amplitude (group 2). In each cell it is possible to check the H and the α_{DFA} values for all four cases.

- $H(\text{Hight Amplitude}) \rightarrow H(\text{Low Amplitude}) =$.

For the **Case 4**, DBS **on** and L-dopa **on**, the most complete Parkinson's treatment, we found that:

- $F_{DFA} \propto n^{\alpha_{DFA}}$, for both conditions, in High and Low Amplitudes (power-law), with $< \alpha_{DFA} >= 0.66$ (Hight Amplitude) and $< \alpha_{DFA} >= 0.61$ (Low Amplitude);
- $H(\text{Hight Amplitude}) \rightarrow H(\text{Low Amplitude}) = 0.69$.

Conclusion

The benefits of chronic DBS in the GPi, Vim and STN nucelli in patients with Parkinson's disease are well-documented. The surgical procedure, in addition to improving the motor symptoms of the disease, reduces the prevalence of pain (musculoskeletal) and improves the discrimination of mechanical sensitivity. To better understand the behavior of these patients who received deep stimulation, and given the subjectivities of the performance of the UPDRS and TRS scales. In this paper, we propose to study the auto-correlation of the speed of resting tremor obtained through a sensor inserted into the index finger of 16 patients, by DFA method and the Shannon Entropy, split into two groups, one with High Amplitude and the other with Low Amplitude Parkinsonian tremor.

Therefore, after all results, we observe that the DFA auto-correlation analysis and the Shannon Entropy, can capture the influence of the treatment of patients with Parkinson's disease, with DBS **on–off** and L-dopa **on–off**. From this statement, in the case where DBS (off) and L-dopa (off) (patients without any treatment), there is a clear transition in F_{DFA} behavior for $n = 20$, better explained to patients in the group 1 (High Amplitudes of tremor), with $H \approx 1.0$ (maximum uncertainty in the position of the laser reading). However, with either one,

DBS or L-dopa **on**, there is a tendency for F_{DFA} transition in $n = 20$ disappear, and at the same time for Hight Amplitude tremor, with H value decreasing from its maximum value. This entire statement is confirmed when DBS (**on**) and L-dopa (**on**), because there is a clear influence on the fluctuation function, F_{DFA}, identifying by long-range power-law auto-correlations, and with $\alpha_{DFA} \approx 0.6$. Also, in this case, looking at the Shannon Entropy, we can notice that its values, $H \approx 0.6$, is less than its maximum, or its maximum uncertainty ($H = 1.0$).

Finally, the auto-correlation exponent α_{DFA} provides insights into the persistence of signals produced by the Parkinson finger tremor, mainly differentiating those in Low and High Amplitude tremor, or even identifying transition of behavior with a typical time scale. Shannon Entropy gives us information about the uncertainty in the position of the tremor, a high value of H informs us that we have a high uncertainty in the signal of this tremor. Therefore, by combining these two techniques we have a better view of the (signal/noise) effects of DBS and L-dopa in all patients with Parkinson's disease, and thus helping to make a better analysis of this health problem.

Data availability

The datasets generated and/or analyzed during the current study are available in the repository www.physionet.org, page https://physionet.org/content/eegmmidb/1.0.0/. And all analyses performed during the study are available from the corresponding author upon request. Therefore, there is no impediment to their transfer and use.

Received: 17 August 2024; Accepted: 12 March 2025
Published online: 24 March 2025

References

1. Groiss, S. J., Wojtecki, L., Südmeyer, M. & Schnitzler, A. Deep brain stimulation in Parkinson's disease. *Ther. Adv. Neurol Disord.* **2**(6), 20–28 (2009).
2. Dovzhenok, A. & Rubchinsky, L. L. On the Origin of Tremor in Parkinson's Disease. *PLoS One* **7**(7), e41598 (2012).
3. Tsai, S.-T. et al. Dorsolateral subthalamic neuronal activity enhanced by median nerve stimulation characterizes parkinson's disease during deep brain stimulation with general anesthesia. *J. neurosurg.* **123**, 1394–1400 (2015).
4. Lee, W.-W. et al. Bilateral deep brain stimulation of the subthalamic nucleus under sedation with propofol and fentanyl. *PLoS One* **11**, e0152619 (2016).
5. França, C., Carra, R. B., Diniz, J. M., Munhoz, R. P. & Cury, R. G. Deep brain stimulation in Parkinson's disease: state of the art and future perspectives. *Arquivos de Neuro-Psiquiatria* **80**, 105–115 (2022).
6. Beuter, A., Titcombe, M., Richer, F., Gross, C. & Guehl, D. Effect of deep brain stimulation on amplitude and frequency characteristics of rest tremor in parkinson's disease. *Thalamus Relat. Syst.* **1**, 203–211 (2001).
7. Alegret, M. et al. Effects of bilateral subthalamic stimulation on cognitive function in parkinson disease. *Archiv. Neurol.* **58**, 1223–1227 (2001).
8. Lee, S. H. et al. Clinical factors and dopamine transporter availability for the prediction of outcomes after globus pallidus deep brain stimulation in parkinson's disease. *Sci. Rep.* **12**, 16870 (2022).
9. Choubdar, H. et al. Neural oscillatory characteristics of feedback-associated activity in globus pallidus interna. *Sci. Rep.* **13**, 4141 (2023).
10. Follett, K. A. The surgical treatment of parkinson's disease. *Ann. Rev. Med.* **51**, 135–147 (2000).
11. Pahwa, R., Wilkinson, S. B., Overman, J. & Lyons, K. E. Bilateral subthalamic stimulation in patients with parkinson disease: long-term follow up. *J. Neurosurg.* **99**, 71–77 (2003).
12. Rodriguez, R. L., Fernandez, H. H., Haq, I. & Okun, M. S. Pearls in patient selection for deep brain stimulation. *Neurol.* **13**, 253–260 (2007).
13. Hariz, M. I., Rehncrona, S., Quinn, N. P., Speelman, J. D. & Wensing, C. Multicenter study on deep brain stimulation in parkinson's disease: an independent assessment of reported adverse events at 4 years. *Movement Disorder. Off. J. Movement Disorder Soc.* **23**, 416–421 (2008).
14. Su, D. et al. Frequency-dependent effects of subthalamic deep brain stimulation on motor symptoms in Parkinson's disease: a meta-analysis of controlled trials. *Sci. Rep.* **8**, 14456 (2018).
15. Oh, M., Kim, H. & Lee, H. K. Medication recommendation for Parkinson's disease based on dynamics of symptom progression. *Sci. Rep.* **14**, 25051 (2024).
16. Krause, M. et al. Deep brain stimulation for the treatment of parkinson's disease: subthalamic nucleus versus globus pallidus internus. *J. Neurol. Neurosurg. Psychiatry* **70**, 464–470 (2001).
17. Lang, A. E. et al. Deep brain stimulation: preoperative issues. *Movement Disord. Off. J. Movement Disorder Soc.* **21**, S171–S196 (2006).
18. Hughes, A. J., Daniel, S. E., Kilford, L. & Lees, A. J. Accuracy of clinical diagnosis of idiopathic parkinson's disease: a clinico-pathological study of 100 cases. *J. Neurol. Neurosurgery Psychiatry* **55**, 181–184 (1992).
19. Rajput, D. Accuracy of clinical diagnosis of idiopathic parkinson's disease. *J. Neurol. Neurosurgery Psychiatry* **56**, 938 (1993).
20. Status and recommendations. on Rating Scales for Parkinson's Disease, M. D. S. T. F. The unified parkinson's disease rating scale (updrs). *Movement Disorder.* **18**, 738–750. https://doi.org/10.1002/mds.10473 (2003).
21. Weaver, F., Follett, K., Hur, K., Ippolito, D. & Stern, M. Deep brain stimulation in parkinson disease: a metaanalysis of patient outcomes. *J. Neurosurg.* **103**, 956–967 (2005).
22. Peto, V., Jenkinson, C. & Fitzpatrick, R. Pdq-39: a review of the development, validation and application of a parkinson's disease quality of life questionnaire and its associated measures. *J. Neurol.* **245**, S10–S14 (1998).
23. Krack, P. et al. Five-year follow-up of bilateral stimulation of the subthalamic nucleus in advanced parkinson's disease. *New England J. Med.* **349**, 1925–1934 (2003).
24. Temel, Y., Blokland, A., Steinbusch, H. W. & Visser-Vandewalle, V. The functional role of the subthalamic nucleus in cognitive and limbic circuits. *Progress Neurobiol.* **76**, 393–413 (2005).
25. PhysioBank, P. Physionet: components of a new research resource for complex physiologic signals. *Circulation* **101**, e215–e220 (2000).
26. Calne, D. & Sandler, M. L-dopa and parkinsonism. *Nature* **226**, 21–24 (1970).
27. Moody, G., Mark, R. & Goldberger, A. Physionet: a web-based resource for the study of physiologic signals. *IEEE Eng. Med. Biol. Magazine* **20**, 70–75. https://doi.org/10.1109/51.932728 (2001).
28. Peng, C. K. et al. Mosaic organization of DNA nucleotides. *Phys. Rev. E* **49**, 1685–1689 (1994).

29. Walleczek, J. *Self-organized biological dynamics and nonlinear control: toward understanding complexity, chaos and emergent function in living systems* (Cambridge University Press, 2006).
30. Zebende, G. F., Fernandez, B. F. & Pereira, M. G. Analysis of the variability in the sdB star KIC 10670103: DFA approach. *Monthly Notices Royal Astronomical Soc.* **464**, 2638–2642 (2016).
31. Zebende, G. F., Oliveira-Filho, F. M. & Leyva-Cruz, J. A. Auto-correlation in the motor/imaginary human EEG signals: A vision about the FDFA fluctuations. *PLOS One* **12** (2017).
32. Oliveira-Filho, F. M., Leyva-Cruz, J. A. & Zebende, G. F. Analysis of the EEG bio-signals during the reading task by DFA method. *Physica A* **525**, 664–671 (2019).
33. Mesquita, V. B., Oliveira-Filho, F. M. & Rodrigues, P. C. Detection of crossover points in detrended fluctuation analysis: An application to EEG signals of patients with epilepsy. *Bioinformatics* https://doi.org/10.1093/bioinformatics/btaa955 (2020).
34. Filho, F. M. O. & de Santana, J. P. C. Difference in the Range of Floating in Individuals Diagnosed with Amyotrophic Lateral Sclerosis: A preliminary study with the rms float function. *International Journal of Research in Engineering and Science* (2022).
35. Oliveira Filho, e. a. Self-regulation in electroencephalographic signals during an arithmetic performance test: an approach with an rms fluctuation function. 15921091210 **9** (2021).
36. Oliveira Filho, F., Ribeiro, F., Cruz, J. L., de Castro, A. N. & Zebende, G. Statistical study of the eeg in motor tasks (real and imaginary). *Phys. A Statist. Mechan. Appl.* **622**, 128802 (2023).
37. Filho, F. M. O. & Zebende, G. F. Temporal coherence in the synchronization of brain electrical activity patterns: An application with the rms fluctuation function. *J. ISSN* **2766**, 2276 (2024).
38. Hartley, R. V. L. Transmission of information. *Bell Syst. Tech. J.* **7**, 535–563 (1928).
39. Shannon, C. E. A mathematical theory of communication. *Bell Syst. Techn. J.* **27**, 623–656 (1948).
40. Brillouin, L. *Science and Information Theory* (Dover Books on Physics (Dover Publications, Incorporated, 2013).
41. Nielsen, M. A. & Chuang, I. L. *Quantum computation and quantum information* (Cambridge university press, 2010).
42. Ali, A., Anam, S. & Ahmed, M. M. Shannon entropy in artificial intelligence and its applications based on information theory. *J. Appl. Emerging Sci.* **13**, 09–17 (2023).
43. Gao, J., Hu, J. & Tung, W.-W. Entropy measures for biological signal analyses. *Nonlinear Dyn.* **68**, 431–444 (2012).
44. Gil, L. M., Nunes, T. P., Silva, F. H., Faria, A. C. & Melo, P. L. Analysis of human tremor in patients with parkinson disease using entropy measures of signal complexity. In *2010 Annual International Conference of the IEEE Engineering in Medicine and Biology*, 2786–2789 (IEEE, 2010).
45. Conforte, A. J., Tuszynski, J. A., Silva, F. A. B. d. & Carels, N. Signaling complexity measured by shannon entropy and its application in personalized medicine. *Frontiers in Genetics* **10**, 461182 (2019).
46. Bakstein, E., Warwick, K., Burgess, J., Stavdahl, Ø. & Aziz, T. Features for detection of parkinson's disease tremor from local field potentials of the subthalamic nucleus. In *2010 IEEE 9th International Conference on Cyberntic Intelligent Systems*, 1–6 (IEEE, 2010).
47. Afsar, O., Tirnakli, U. & Kurths, J. Entropy-based complexity measures for gait data of patients with parkinson's disease. *Chaos: An Interdisciplinary Journal of Nonlinear Science* **26** (2016).
48. Vaillancourt, D. E. & Newell, K. M. The dynamics of resting and postural tremor in parkinson's disease. *Clin. Neurophysiol.* **111**, 2046–2056 (2000).
49. Jost, L. Entropy and diversity. *Oikos* **113**, 363–375 (2006).
50. Mishra, S. & Ayyub, B. M. Shannon entropy for quantifying uncertainty and risk in economic disparity. *Risk Analy.* **39**, 2160–2181 (2019).
51. Papadimitriou, C., Karamanos, K., Diakonos, F., Constantoudis, V. & Papageorgiou, H. Entropy analysis of natural language written texts. *Phys. A Statist. Mechan. Appl.* **389**, 3260–3266 (2010).
52. Schneider, T. Information theory primer with an appendix on logarithms (PDF version). Tech. Rep., MIT (2018). https://doi.org/10.13140/2.1.2607.2000.

Acknowledgements

Florencio Mendes Oliveira Filho thanks SENAI CIMATEC UNIVERSITY and the National Council for Scientific and Technological Development (CNPq 25/2021) scholarship 150655/2022-3. Zebende acknowledges financial support from CNPq Grant 310136/2020-2. We send a special thank to Flora Leite Primo Oliveira (Descriptive art), Irles Azevedo Oliveira Sá Teles (Social Worker) and Carlos Eduardo de Paula (Radiologist) for their valuable contributions.

Author contributions

All researchers participated in all aspects of the manuscript construction.

Additional information

Correspondence and requests for materials should be addressed to F.M.O.F.

Reprints and permissions information is available at www.nature.com/reprints.

Publisher's note Springer Nature remains neutral with regard to jurisdictional claims in published maps and institutional affiliations.